NASA TECHNICAL MEMORANDUM

NASA TM X-2919

NASA TM X-2919

FLIGHT VELOCITY EFFECTS ON JET NOISE OF SEVERAL VARIATIONS OF A 48-TUBE SUPPRESSOR INSTALLED ON A PLUG NOZZLE

by Richard R. Burley and Verlon L. Head

Lewis Research Center
Cleveland, Ohio 44135

NATIONAL AERONAUTICS AND SPACE ADMINISTRATION • WASHINGTON, D. C. • FEBRUARY 1974

1. Report No.	2. Government Accession No.	3. Recipient's Catalog No.
NASA TM X-2919		

4. Title and Subtitle	5. Report Date
FLIGHT VELOCITY EFFECTS ON JET NOISE OF SEVERAL VARIATIONS OF A 48-TUBE SUPPRESSOR INSTALLED ON A PLUG NOZZLE	January 1974
	6. Performing Organization Code

7. Author(s)	8. Performing Organization Report No.
Richard R. Burley and Verlon L. Head	E-7513
	10. Work Unit No. 501-24

9. Performing Organization Name and Address	11. Contract or Grant No.
Lewis Research Center National Aeronautics and Space Administration Cleveland, Ohio 44135	
	13. Type of Report and Period Covered: Technical Memorandum

12. Sponsoring Agency Name and Address	14. Sponsoring Agency Code
National Aeronautics and Space Administration Washington, D.C. 20546	

15. Supplementary Notes

16. Abstract

Because of the relatively high takeoff speeds of supersonic transport aircraft, it is important to know if the flight velocity affects the noise level of suppressor nozzles. To investigate this, a modified F-106B aircraft was used to conduct a series of flyover and static tests on a 48-tube suppressor installed on an uncooled plug nozzle. Comparison of flyover and static spectra indicated that flight velocity had little effect on the noise suppression of the 48-tube suppressor configuration. However, flight velocity adversely affected noise suppression of the 48-tube suppressor with an acoustic shroud and plug installed.

17. Key Words (Suggested by Author(s))	18. Distribution Statement
Flight velocity effect; Jet noise suppressors; Nozzle thrust; Propulsion systems; Plug nozzle	Unclassified - unlimited Cat. 28

19. Security Classif. (of this report)	20. Security Classif. (of this page)	21. No. of Pages	22. Price*
Unclassified	Unclassified	37	$3.00

* For sale by the National Technical Information Service, Springfield, Virginia 22151

Page Intentionally Left Blank

FLIGHT VELOCITY EFFECTS ON JET NOISE OF SEVERAL VARIATIONS OF A 48-TUBE SUPPRESSOR INSTALLED ON A PLUG NOZZLE

by Richard R. Burley and Verlon L. Head

Lewis Research Center

SUMMARY

Because of the relatively high takeoff speeds of supersonic transport aircraft, it is important to know if the flight velocity affects the noise level of suppressor nozzles. To investigate this, a series of flyover and static tests were conducted on a 48-tube suppressor installed on an uncooled plug nozzle. The effects of incorporating an acoustically treated shroud and plug and of incorporating scoops also were studied. The tests were conducted using an F-106B aircraft modified to carry two underwing nacelles each containing a calibrated J85-GE-13 turbojet engine. Data were taken over a range of J85 engine power settings that resulted in relative jet velocities from 410 to 620 meters per second (1350 to 2050 ft/sec) at static conditions and from 250 to 500 meters per second (820 to 1650 ft/sec) for flyover conditions.

Comparison of the adjusted flyover and static spectra at the acoustic angle that resulted in peak flyover noise indicated that flight velocity had little effect on the noise suppression of the 48-tube suppressor. However, flight velocity had an adverse effect on the noise suppression of the 48-tube suppressor with the acoustic shroud and plug installed. The frequency spectrum of the 48-tube suppressor in flyover contained only a small amount of low-frequency noise but as much high-frequency noise as the baseline nozzle, with the peak noise occurring at a frequency of 4000 hertz. Installing the acoustic shroud reduced the noise by as much as 14 decibels at a frequency of 4000 hertz.

When the acoustic data from the flyover tests were scaled from J85 engine size (0.23 scale) to a full-scale four-engine aircraft and extrapolated to a sideline distance of 648 meters (2128 ft) from an altitude of 305 meters (1000 ft), the bare 48-tube suppressor reduced the noise level relative to the baseline nozzle by 5 effective perceived noise decibels (EPNdB). This noise reduction was achieved with a thrust penalty of about 10.5 percent. The greatest amount of noise reduction, 15 EPNdB, was achieved by incorporating the scoops along with the acoustic shroud and plug. However, it was achieved with a thrust penalty of 34 percent.

INTRODUCTION

During takeoff of supersonic transport aircraft, the dominant noise source is the high-velocity jet issuing from the exhaust nozzle. Investigations of acoustic characteristics of both unsuppressed and suppressor-type exhaust nozzles generally have been made at static conditions (cf. refs. 1 to 3). However, the takeoff speed of supersonic aircraft can be as high as Mach 0.35 when maximum sideline noise is reached. Thus, it is important to know whether the flight velocity affects the noise and thrust of exhaust nozzles.

To gain some insight into this question, a series of flyover and static tests are being conducted on unsuppressed and suppressor-type exhaust nozzles. Some preliminary results are reported in references 4 and 5. In reference 6 an investigation of three basic types of unsuppressed nozzles shows that flight velocity has a beneficial effect on the noise suppression of an auxiliary inlet ejector nozzle. Results for a 32-spoke suppressor (ref. 7) and for a 12-chute suppressor configuration (ref. 8) have shown an adverse effect of flight velocity on the noise suppression of these configurations.

Another attractive type of suppressor is the multitube configuration. The present investigation was conducted to determine whether flight velocity affects the noise and thrust of a 48-tube suppressor installed on an uncooled plug nozzle. The suppressor was tested with no shroud, with an acoustically lined shroud, and with both an acoustically treated shroud and plug. The effect of installing scoops also was studied.

The tests were conducted using an F-106B aircraft modified to carry podded engines mounted near the aft lower surface of the wing with the exhaust nozzles extending beyond the wing trailing edge. The primary jet exhaust was provided by calibrated turbojet engines (J85-GE-13). The flyovers were conducted at an altitude of 91 meters (300 ft) and a Mach number of 0.4. Acoustic measurements were taken from a ground station directly beneath the flightpath. For static tests, the acoustic measurements were taken at a radial distance of 30.48 meters (100 ft) from the nozzle. Data were taken over a range of J85 engine power settings from part throttle to military rpm. These settings gave a range of relative jet velocities from 410 to 620 meters per second (1350 to 2050 ft/sec) at static conditions and from 250 to 500 meters per second (820 to 1650 ft/sec) for flyover conditions.

APPARATUS AND PROCEDURE

Test Facility

Flyover and static tests were conducted with an F-106B aircraft modified to carry

two underwing nacelles. The aircraft in flight is shown in figure 1. A schematic view of the nacelle-engine installation is presented in figure 2. The 63.5-centimeter (25-in.) diameter nacelles were located at approximately 32 percent semispan with the exhaust nozzles extending beyond the wing trailing edge. Since the nozzle would interfere with normal elevon movement, a section of the elevon immediately above each nacelle was cut out and rigidly attached to the wing. Each nacelle contained a calibrated J85-GE-13 afterburning turbojet engine. The nacelles had normal shock inlets with blunted cowl lips for the flyover tests. Secondary air to cool the engine and afterburner was supplied from the inlet and was controlled at the periphery of the compressor face by a calibrated rotary valve. For the static tests, the blunted cowl lips were replaced with a bell-mouthed inlet, as shown in figure 3.

Each nacelle was attached to the wing by two links normal to the nacelle axis, and the axial force was measured by a load cell attached to the wing as shown in figure 2. An accelerometer in the nacelle allowed the load cell to be compensated for acceleration. The axial force transmitted to the compensated load cell can be divided into two parts: (1) nacelle drag forward of the research nozzle, referred to as the tare force; and (2) research nozzle gross thrust minus drag. Gross thrust minus drag is determined by adding the tare force to the compensated load cell reading. The tare force was zero for the static test (ref. 6). For flyover tests, the tare force is the sum of the ram drag plus the skin friction drag on nacelle and strut (ref. 6).

Baseline Nozzle

The baseline nozzle used for this study was an unsuppressed plug nozzle shown in figure 4(a) installed on the aircraft. A schematic is shown in figure 4(b). The baseline nozzle consisted of a 10° half-angle conical plug body and a primary flap with a 14° trailing edge. A plug nozzle generally has a translating outer shroud which is retracted for efficient operation at the low pressure ratios for takeoff conditions. The present configuration simulates the shroud in this position. Further details of this nozzle design are given in reference 9. Acoustic and thrust results for flyover conditions are presented in reference 6.

Suppressor Configurations

Details of suppressor configuration components are shown in figure 5. The 48-tube primary, installed on the plug nozzle just discussed, is shown in figure 5(a-1). A schematic is shown in figure 5(a-2). The geometric throat of this primary was at about

the same axial station as the exit plane for the primary flap of the plug nozzle. A plug nozzle was selected for the suppressor tests because it provides good aerodynamic performance, its mechanical systems are relatively simple, and the plug body provides a place to stow retractable noise suppressors.

The 48-tube configuration had a blunt base (fig. 5). The tubes were arranged in six clusters, called nozzle boxes. Each nozzle box contained eight tubes. For each nozzle box, the ratio of the area enclosed within the perimeter of a nozzle box to the effective exhaust area of the tubes in this nozzle box is about 2.5. The tubes were 10.15 centimeters (4 in.) long, resulting in a ventilation factor (ratio of side flow area to base area per nozzle box) of 0.3. There were also six triangular-shaped openings (one opening between each of the nozzle boxes) through which about one-third of the primary flow was discharged.

A major consideration dictating the shape of this configuration was that, in concept, the tubes were stowable inside the plug body. Three of the nozzle boxes would slide inward and forward on tracks and be stowed forward in the plug. The other three nozzle boxes would fold into the plug by means of a pivot. The nozzle box side walls (fig. 5(a-1)) would then cover the tubes and become part of the plug surface. This stowable concept imposed limitations on the configuration which may have degraded its acoustic and thrust performance.

The scoops installed on the 48-tube primary are shown in figure 5(b). There were six scoops located around the periphery of the nozzle. The scoop angle was 25°, and the downstream ends of the scoops were in the same plane as the exit of the 48-tube primary.

The 48-tube primary with the scoops and the acoustically treated shroud and acoustically treated plug is shown in figure 5(c). The acoustically treated shroud and plug were the same as those used in reference 8. The acoustic treatment consisted of a perforated plate adjacent to the hot jet, a bulk absorber, and a solid backing plate. Baffle disks, used for structural integrity, also kept the bulk absorber from axial movement and served as resonator walls. The stainless-steel perforated plate was 0.079 centimeter (0.031 in.) thick and had 0.198-centimeter (0.078-in.) diameter holes and a 23 percent open area. The bulk absorber was 0.028-centimeter (0.011-in.) diameter stainless-steel wire mesh that filled each cavity to a density of 322 kg/m^3 (20 lb/ft^3).

The acoustic shroud which had an outer diameter of 63.5 centimeters (25 in.) to be consistent with the nacelle diameter, was 56.7 centimeters (22.3 in.) long to simulate a translating shroud in its supersonic cruise position. It had a maximum cavity depth of 2.97 centimeters (1.17 in.), which resulted in a shroud exit diameter of 57.18 centimeters (22.51 in.). The outer surface of the shroud had a boattail angle of 15° and a boattail juncture radius of 0.24 nacelle diameter. The absorber probably will act as a broadband absorber since it is of the bulk type and is exposed to high gas flow velocities and high sound pressure levels (ref. 10).

The acoustic plug was truncated to 80 percent of its full length. This amount of truncation should not significantly affect thrust performance (ref. 9). The acoustic treatment applied to the exposed surface of the plug resulted in a lining length of 75 centimeters (29.5 in.). The cavity depth varied from a maximum of 15 centimeters (5.8 in.) to a minimum of 1.55 centimeters (0.6 in.). This liner will also probably act as a broadband absorber.

Instrumentation

An onboard digital data system was used to record pressures, temperatures, and load cell output on magnetic tape. It had the capability of recording 578 parameters in 11.5 seconds (ref. 11). A flight-calibrated test boom located on the aircraft nose was used to determine free-stream static and total pressure, aircraft angle of attack, and yaw angle. Aircraft altitude was determined by an onboard radio altimeter and a barometric altimeter, along with ground-based radar. Aircraft velocity was obtained from a calibrated Mach meter the output of which was sampled and recorded six times in 11.5 seconds by an onboard digital data system.

Engine airflow was determined by using the calibrated results from reference 12, along with measurements of engine speed and total pressure and temperature at the compressor face. Fuel flows were obtained from calibrated flowmeters. Total temperature T_8, total pressure P_8, and effective area at the primary nozzle exit A_8 were obtained by using the values of engine airflow and fuel flow, the measured values of total pressure and temperature at the turbine discharge, and afterburner temperature rise and pressure drop calibration results from reference 12. Calibration of the secondary-flow-valve pressure drop and position were used to determine secondary airflow.

Total pressure and temperature of the secondary air were obtained from the probes shown in figure 6. Static pressures on the base plate of the primary nozzle are shown in figure 7.

The noise-measuring instrumentation is shown in the block diagram of figure 8. The microphone was a 2.54-centimeter (1-in.) diameter ceramic type. Frequency response of the microphone was flat to within ± 2 decibels for grazing incidence over the frequency range used. The output of the microphone was recorded on a two-channel direct-record tape recorder. The entire system was calibrated for sound level in the field before and after each test with a conventional tone calibrator. The tape recorder was calibrated for linearity with a "pink" noise (constant energy per octave) generator.

The flyover signal, recorded on magnetic tape, was played back through 1/3-octave-band filters and then reduced to a digital form (fig. 8(b)). The averaging time used for data reduction was 0.1 second. The digital results were recorded on a tape. The time

history of each flyover (in terms of PNL) and three associated frequency spectra (at peak PNL and 10 PNdB down on either side) were automatically plotted.

The static signal recorded on magnetic tape was played back through 1/3-octave-band filters, and the spectra were automatically plotted (fig. 8(c)). The averaging time used for data reduction was 1/8 second. The plotted results were converted into digital form and recorded on tape.

Meteorological conditions, in terms to dry-bulb and dewpoint temperatures, wind speed and direction, and barometric pressure were recorded periodically throughout the test. Wind speeds were less than 5.144 meters per second (10 knots) during the tests.

Procedure

The microphone stations for the acoustic measurements are shown in figure 9 for static conditions. The portable microphone was positioned 1.22 meters (4 ft) above the concrete surface and was oriented to receive the acoustic pressure waves at normal incidence (fig. 9(a)). The microphone was fitted with a wind screen that caused no loss of signal. The acoustic measurements were made at a radial distance of 30.48 meters (100 ft) from the nozzle exit in increments of 10° over a 90° sector (fig. 9(b)). During the measurements, the main J75 engine was at idle power. The J85 engine in the nacelle containing the research nozzle was operated over a range of power settings, and the J85 engine in the other nacelle was shut off.

Background noise level for the static tests were determined with both J85 engines shut off, the J75 engine at idle power, and external cooling air on. It was necessary to supply air from an external source to cool the J85 engine when it was operating at military power setting. The air was supplied from an air start cart which was located on the far side of the aircraft, as shown in figure 10. The supply line went from the start cart to the J85 engine, and the air was directed around the engine through a nozzle (fig. 3). The J75 engine had to be operating when static data were taken because it supplied the electrical power for the onboard digital data system.

The background noise spectra (i.e., with the J75 engine at idle power and the external air on) at acoustic angles of 30° to 70° are presented in reference 4. These spectra were adjusted to a standard day but not to free-field conditions. After adjustment to free-field conditions, the spectra levels gradually increased to about 87 decibels at a frequency of 1000 hertz. They remained fairly constant until, at a frequency of 2500 hertz, they started to decrease and reached a level of about 77 decibels at a frequency of 10 000 hertz. The background noise levels are sufficiently low so they do not interfere with the noise from the suppressor nozzles.

Acoustic measurements of the flyover noise were made from a ground station directly

beneath the flightpath. The position of the microphone is shown in figure 11(a). It was positioned 1.22 meters (4 ft) above the concrete surface. The microphone, which was fitted with a wind screen that caused no loss of signal, was oriented to receive the acoustic pressure wave at grazing incidence.

The geometry of the flyover is shown in figure 11(b). As the aircraft travels along its flightpath, the direct ray distance from the nozzle to the microphone R_p continuously changes. The angle between the direct ray and the jet exit centerline, referred to as the acoustic angle θ, also changes. The values of R_p and θ are related to the sound data taken at a particular instant of time by having a ground observer manually record a signal on the tape (fig. 8(a)) as the aircraft passes directly over the microphone.

The flyovers were conducted at a Mach number of 0.4 and at an altitude of 91 meters (300 ft). (Ref. 6 discusses the reasons for selecting this particular altitude.) The main engine of the aircraft was at idle power while the data were being recorded. The J85 engine in the nacelle that contained the research nozzle was operated at military and part power settings. The J85 engine in the opposite nacelle was shut off and allowed to windmill.

Background noise level during flyover was determined with the main engine at idle power and both J85 engines shut off and allowed to windmill. The results adjusted to a standard day but not to free-field conditions are presented in reference 6. An acoustic angle of 115° gave a peak background noise level of 99 PNdB adjusted to free-field conditions. (As is shown in the section Acoustic Characteristics, the suppressor nozzles reach their peak noise level at acoustic angles of 70° or less.) The associated frequency spectrum has a fairly flat shape over most of the frequency range. The level, adjusted to free field, is about 70 decibels at frequencies below about 2000 hertz and decreases to a value of about 57 decibels at a frequency of 10 000 hertz. These levels are sufficiently low so they do not interfere with the noise from the suppressor nozzles.

RESULTS AND DISCUSSION

Acoustic Characteristics

To investigate whether flight velocity affects the noise of the 48-tube suppressor configurations, the measured flyover and static spectra were adjusted to comparable conditions: 30.48 meters (100 ft) from the nozzle in the free field on a standard day. The Doppler frequency shift also was accounted for in the flyover and caused a maximum frequency shift of one 1/3-octave band. Details of the adjustments are given in reference 6. The adjusted flyover and static spectra were then compared at a constant relative jet velocity of 504 meters per second (1654 ft/sec) and for the acoustic angle that

resulted in peak flyover noise. Significant differences between these adjusted spectra would be attributed to flight velocity effects.

In making the comparison, the greatest emphasis should be placed on the data at frequencies between 160 and 5000 hertz. At frequencies below 160 hertz, the short integration time, the narrowness of the frequency bands, and the rapidly changing conditions of the flyover all combine to give results that are not reliable. At frequencies above 5000 hertz, the acoustic signal received at the ground station quite possibly was below the noise floor of the recording equipment (ref. 13). Values of the atmospheric absorption coefficient are very large at these high frequencies and multiply the noise floor to unrealistically high noise levels in adjusting the data to 30.48 meters (100 ft).

The flyover and static spectra for the 48-tube suppressor nozzle are compared in figure 12. There is very close agreement between the spectra, resulting in an overall sound pressure level (OASPL) and a perceived noise level (PNL) that were about the same for the flyover as for the static spectrum. This suggests that flight velocity had little effect on noise suppression of the 48-tube primary.

The flyover and static spectra for the 48-tube suppressor nozzle with the acoustically treated shroud and plug are compared in figure 13. The flyover spectrum is considerably above the static spectrum over most of the frequency range. This results in an OASPL about 6 decibels greater and a PNL about 7 PNdB greater for the flyover than for the static spectrum. It suggests that flight velocity had an adverse effect on noise suppression with this configuration.

In an attempt to increase suppression and to reduce the drag on the baseplate, scoops were installed on the 48-tube suppressor with the acoustically treated shroud and plug. The flyover and static spectra for this configuration are compared in figure 14. The flyover spectrum is again considerably above the static spectrum over most of the frequency range. This results in an OASPL about 4 decibels greater and a PNL about 4.5 PNdB greater for the flyover than for the static spectrum. Thus, flight velocity also adversely affected this configuration but to a lesser extent than without the scoops.

Another indication of flight velocity effect is directivity and peak noise level. Figure 15 shows the variation in perceived noise level with acoustic angle during a typical flyover at an altitude of 91 meters compared with that predicted from static data extrapolated to a 91-meter sideline. Figure 15(a) shows the results for the 48-tube suppressor nozzle. The flyover noise level reached a peak value of about 114 PNdB at an angle of about 70°. The static results correctly predicted both the peak noise level and the angle at which it occurred. Figure 15(b) shows the results for the 48-tube suppressor with the acoustic shroud and plug. The flyover noise level reached a peak value of about 105 PNdB at an angle of about 25°. The static results predicted a higher peak level (110 PNdB) occurring about 45° farther away from the jet axis. Figure 15(c) shows the results for the 48-tube suppressor with scoops as well as the acoustic shroud and plug. The flyover

noise level reached a peak value of about 105 PNdB at an angle of about 40°. Again, the static results predicted a higher peak value (110 PNdB) occurring about 20° farther away from the jet axis. Thus, while the static results correctly predicted the peak noise level and associated acoustic angle for the bare suppressor nozzle, this was not the case when the acoustic shroud and plug were installed. Then the static results predicted a higher peak value occurring farther away from the jet axis.

The results of the flyover tests for all the suppressor configurations are presented in figure 16 in terms of the variation in perceived noise level with acoustic angle. For comparison, the results for the unsuppressed plug nozzle, used as the baseline nozzle, are also shown. The results are presented at a relative jet velocity of 502 meters per second. The background noise level, discussed in the section APPARATUS AND PROCEDURE, is also shown.

The baseline nozzle had a peak noise level of 115 PNdB occurring at an acoustic angle of 40°. Peak noise level of the 48-tube primary was about the same as that of the baseline nozzle but occurred about 20° farther from the jet axis. Incorporating the acoustic shroud and plug resulted in a substantial reduction of 9 PNdB in the peak noise level and shifted it 40° closer to the jet axis when compared with the 48-tube primary. Most of the noise reduction, 7 PNdB, probably was caused by the acoustic shroud since the acoustic plug reduced peak noise level by about 2 PNdB. The suppression achieved by the acoustic plug is based upon comparing the peak noise level of the configuration with the scoops plus acoustic shroud (116.5 PNdB) to that of the configuration with the scoops plus acoustic shroud and acoustic plug (114.5 PNdB). Theoretically (ref. 10), a greater amount of attenuation could be achieved by having the treated surface of the shroud more parallel to the treated surface of the plug (i.e., rotate the shroud toward the plug). The effect this would have on thrust performance is discussed in the section Thrust Characteristics.

Also shown in figure 16 is the effect of installing the scoops. The purposes of the scoops were (1) to reduce the drag on the baseplate to which the 48 tubes were attached by forcing external air into the base region, and (2) to increase noise suppression by promoting rapid mixing between the elemental jets and the ambient air and/or in the "mixing" region of the coalesced jet. Although the scoops had a large effect on noise directivity, they had only a small effect on noise suppression.

The results just discussed were for a constant relative jet velocity. The effect of decreasing the relative jet velocity on peak flyover noise level is shown in figure 17. By comparing the results for a particular suppressor configuration to that for the baseline nozzle, the effectiveness of that particular suppressor as a function of relative jet velocity can be determined. Reducing the relative jet velocity adversely affects the suppression of the 48-tube primary. No suppression was achieved below a relative

jet velocity of about 500 meters per second (1640 ft/sec). For the other configurations, reducing the relative jet velocity did not markedly affect suppression effectiveness.

For all configurations, however, a noise floor is being reached. This noise floor is different than the one previously mentioned, which was the result of the aircraft flying over with the main engine at idle power and both J85 engines shut off and allowed to windmill. This new noise floor is probably the result of internally generated noise from the J85 engine. This noise is considered to be associated with the highly turbulent flow inside the engine tailpipe and exhaust nozzle (ref. 14). Since this noise is proportional to the sixth power of jet velocity rather than the eight power, it will dominate at low jet velocities.

There seem to be two levels to this noise floor (fig. 17). The bare 48-tube suppressor and the baseline nozzle are associated with the higher level. This suggests that the bare 48-tube suppressor is not any more effective in suppressing internally generated noise than the baseline nozzle. Furthermore, the increased surface area of the 48-tube suppressor is a liability because it results in an increase in the scrubbing noise relative to the baseline nozzle with its smaller surface area. The lower level consists of the suppressor configurations that have acoustically treated surfaces (i.e., acoustically treated shroud and/or plug). This suggests that the acoustic surfaces might be effective in suppressing some of the internally generated noise. The bare 48-tube suppressor with scoops also is associated with the lower level for reasons that are not yet known.

The 48-tube suppressor belongs to a large class of suppressors, called "mixing nozzles," which subdivide the jet exhaust into many elemental jets having the same total effective exit area as the unsuppressed nozzle. Jet noise radiated from these nozzles has a composite spectrum. The high-frequency portion is considered to be the noise generated close to the nozzle exit plane by the mixing of the elemental jets with the ambient air. The low-frequency portion is considered to be the noise generated after the elemental jets have merged into a large single jet farther downstream of the nozzle exit.

The flyover spectra for the 48-tube suppressor and its associated configurations are presented in figure 18 along with the spectrum for the baseline nozzle. The results are shown for a relative jet velocity of 502 meters per second and at the acoustic angle that gave peak flyover noise for the baseline nozzle (40°). The spectrum for the bare 48-tube primary contains only a small amount of low-frequency noise compared to that for the baseline nozzle (fig. 18(a)), suggesting that a considerable amount of external air was entrained into the large single jet thereby reducing its velocity. In the 320-hertz band, for example, a reduction of 16 decibels occurred. The bare 48-tube suppressor contains as much high-frequency noise as the baseline nozzle, suggesting that a considerable amount of mixing of the elemental jets with the surrounding air has occurred. The high-frequency noise peaked at about 4000 hertz. Incorporating the acoustic shroud and plug resulted in lowering the spectrum level over a wide range of frequencies (fig. 18(a)).

The reduction amounted to 14 decibels at a frequency of 4000 hertz. The reduction was caused entirely by the acoustic shroud since installing the acoustic plug had little effect on the suppression (fig. 18(b)). The acoustic shroud acted as a broadband absorber because the absorption material was of the bulk type and because of the high sound pressure levels and high gas flow velocities to which the liner was exposed. Installation of the scoops apparently did not promote any significant increase in the amount of mixing either between the elemental jets and the surrounding air or in the "mixing" region of the coalesced jet (fig. 18(c)). The scoops had no marked effect on the frequency spectrum in the region of greatest reliability (at frequencies between 160 and 5000 Hz).

Thrust Characteristics

In addition to acoustic characteristics, thrust characteristics also are important. Thrust performance for all the suppressor configurations is presented in figure 19 in terms of nozzle gross thrust coefficient as a function of nozzle pressure ratio. Values of relative jet velocity are also indicated on the abscissas. To determine the thrust penalty, results for the baseline nozzle also are shown. The figure contains a table showing the ratio of base pressure drag to ideal primary thrust for some of the configurations.

Thrust performance at static conditions is shown in figure 19(a). The baseline nozzle has a gross thrust coefficient of 0.99 at a nozzle pressure ratio of 2.1. Installing the 48-tube suppressor lowered the thrust coefficient to 0.91, which is an 8 percent reduction from the baseline nozzle at a pressure ratio of 2.1. Two factors contribute to this thrust loss. One is the drag caused by the base pressures being lower than ambient. For the bare 48-tube configuration, base pressure drag caused only about a 2 percent loss in thrust (see table). The other factor is the increased wetted surface area (excluding the base area) of the 48-tube suppressor over that of the baseline nozzle, which resulted in decreased internal thrust. This probably accounted for the remaining 6 percent of the thrust loss.

Installing the acoustic shroud lowered the thrust coefficient to 0.807, a 12.3 percent reduction from the bare 48-tube suppressor at a pressure ratio of 2.1. About 8 percent of this reduction was caused by base pressure drag. The shroud exit area was considerably greater than that required to properly expand the primary flow at low values of nozzle pressure ratio. This greater exit area, combined with insufficient entrainment of external air to prevent the primary flow from overexpanding, caused the base pressures to be lower than ambient. A thrust loss also was caused by the primary jets in the outer row of the 48 tubes impinging on the convergent surface of the acoustic shroud. For these configurations, thrust loss is not markedly affected by reducing nozzle pressure ratio.

Thrust performance at flyover conditions is presented in figure 19(b). The baseline nozzle has a gross thrust coefficient of 0.965 at a pressure ratio of 2.4. Installing the 48-tube suppressor lowered the thrust coefficient to 0.862, a 10.5 percent reduction from the baseline nozzle at a pressure ratio of 2.4. About 6 percent of this reduction was caused by base pressure drag (see table). Thrust loss relative to the baseline nozzle increased slightly as nozzle pressure ratio decreased. Incorporating the acoustic shroud and plug lowered the thrust coefficient to 0.735, a 14.5 percent thrust loss from the bare 48-tube suppressor at a nozzle pressure ratio of 2.4. The loss is almost entirely from the shroud, which caused the primary flow to be overexpanded and resulted in a base pressure drag of about 14 percent (see table). Thrust loss relative to the bare 48-tube suppressor was not significantly affected by decreasing the nozzle pressure ratio. Incorporating the scoops on the bare 48-tube suppressor lowered the thrust coefficient to 0.717 from 0.862, about a 15 percent reduction at a pressure ratio of 2.4. The scoops were expected to force external air into the base region, thereby reducing the base pressure drag. However, the base drag did not decrease with the addition of the scoops (see table). The thrust loss relative to the bare 48-tube suppressor increased considerably as nozzle pressure ratio decreased.

Another important question concerns the effect of flight velocity on the thrust coefficient of the suppressor configurations. This effect is shown in figure 20, which was obtained by comparing the static and flyover results from figure 19. Figure 20(a) shows the comparison for the bare 48-tube suppressor. Flight velocity had a large adverse effect on the thrust coefficient of this configuration at high nozzle pressure ratios (a decrease of 5.2 percentage points at a nozzle pressure ratio of 2.3). This result suggests that the ventilation for this configuration was much worse for flyover than for static conditions probably because of the blunt base. The adverse effect became even more pronounced as the pressure ratio decreased.

Installing an acoustic shroud and plug on the 48-tube primary, as mentioned in connection with figure 19, caused a thrust loss at both static and flyover conditions principally because the primary flow was overexpanded. As shown in figure 20(b), the effect of flight velocity was to increase the overexpansion loss - a decrease of 8.5 percentage points at a pressure ratio of 2.3. The adverse effect increased as pressure ratio decreased.

As just mentioned, the acoustically treated shroud caused a large thrust loss because the primary flow was overexpanded. The overexpansion could be reduced by shortening the shroud length. But this would reduce the lining length which, in turn, would decrease the attenuation. A method of decreasing overexpansion without decreasing attenuation would be to rotate the shroud toward the plug. For no overexpansion, the separation distance between the treated surfaces of the shroud and plug would be such as to maintain a constant annular area. This, as mentioned in connection with figure 16,

would result in increased attenuation. Although rotating the shroud would increase the boattail surface and thereby increase drag, the thrust loss due to overexpansion would decrease. So there is probably some configuration that minimizes the total thrust loss. This configuration would have a greater amount of attenuation than the existing configuration.

Suppressor Effectiveness

The suppressor configurations tested were 0.23-scale (J85 engine size) models for a supersonic transport engine. To determine suppressor effectiveness, acoustic data from the flyover tests were scaled to full size (four 267-kN (60 000-lbf) thrust engines). This scaling was done by using the Strouhal number relation (ref. 15) and assuming that both the 0.23-scale and full-scale engines were operating with identical primary gas conditions of pressure ratio, total temperature, and gas composition. It was further assumed that the 0.23-scale and the full-scale suppressors were exposed to identical flight velocities and were influenced in an identical manner by flight velocity.

After being adjusted to free-field conditions (ref. 6) and to standard-day conditions (simplified procedure outlined in ref. 16), the full-scale acoustic results were extrapolated to a sideline distance of 648 meters (2128 ft) from an altitude of approximately 305 meters (1000 ft). This extrapolation accounted for inverse-square radiation and atmospheric absorption. For this full-scale spectrum, which occurs at a particular instant of time, values of OASPL and PNL can be obtained. The entire procedure is then repeated for a number of time points. Finally, a time history, in terms of PNL, can be constructed and a value of EPNL can be obtained (procedure outlined in ref. 16).

Suppressor effectiveness for all the configurations is presented in figure 21 in terms of effective perceived noise level (EPNL) suppression (in EPNdB) as a function of percent thrust loss (relative to the baseline nozzle). The results are shown for a Mach number of 0.4 and a nozzle pressure ratio of 2.4 (relative jet velocity, 533 m/sec (1750 ft/sec)). The 48-tube primary is about as effective a noise suppressor (5 EPNdB suppression for 10.5 percent thrust loss) as the 48-tube primary with acoustic shroud and plug (14 EPNdB suppression for 24 percent thrust loss). The largest amount of suppression was 15 EPNdB and was achieved by using the scoops along with the acoustic shroud and plug. However, it was achieved with a thrust loss of 34 percent.

In the preceding discussion, suppression was given in terms of a parameter called effective perceived noise level (EPNL), the units of which are EPNdB. This parameter accounts for suppression due to the distance between the noise source and the observer. It also accounts for the duration of the noise as the aircraft flies past the observer - a longer duration noise being more annoying and therefore less favorable than one of shorter

duration. The amount that each of these factors contributes to the suppression of the 48-tube suppressor is shown in figure 22. Also shown is the effect that scaling has on suppression. A suppression of less than 1 PNdB was achieved with the 0.23-scale 48-tube suppressor when it was flown over the measuring station at an altitude of 91 meters (300 ft) and a Mach number of 0.4. Although scaling to full size resulted in the 48-tube suppressor becoming noisier than the baseline nozzle by about 2 PNdB, this might be in error (due to experimental measurement difficulties that will be discussed).

The effect that distance has on suppression was determined by using the full-scale results that had been extrapolated to the sideline distance of 648 meters from an altitude of 305 meters. A suppression of 3 PNdB was achieved, compared to an increase of a PNdB when the full-scale suppressor was flown at an altitude of 91 meters directly over the measuring station. So the 48-tube suppressor benefits by 5 PNdB when the distance between the noise source and the observer is increased. This is because the spectrum of the suppressor contains more high-frequency noise than does the spectrum of the baseline nozzle and the atmosphere selectively attenuates the high-frequency noise.

The last effect studied was that of time duration. Noise from the suppressor nozzle has a shorter time duration, and therefore the annoyance from this factor is less, by 2 EPNdB, than noise from the baseline nozzle. The noise level of the suppressor nozzle rises and falls more rapidly with time than does the noise level of the baseline nozzle.

Earlier in this section, it was mentioned that the increase in suppression might not be a real effect. Instead it might be the result of the full-scale spectrum being inaccurate at the higher frequencies where the noise floor is above the acoustic signal. Since the scaling factor is 0.23, the measured data at a frequency of 10 000 hertz scale to 2300 hertz. Full-scale noise levels at frequencies greater than 2300 hertz were obtained by extrapolation of the measured spectra.

Since the effect of scaling on suppression might be in error, this same uncertainty affects the absolute levels of suppression due to distance and duration. However, the relative differences probably are correct.

SUMMARY OF RESULTS

A series of flyover and static tests were conducted on a 48-tube suppressor installed on an uncooled plug nozzle. The effects of incorporating an acoustically treated shroud and plug and of incorporating scoops also were studied. The primary jet exhaust was provided by a calibrated turbojet engine. Data were taken over a range of power settings which resulted in relative jet velocities between 250 and 500 meters per second (820 to 1650 ft/sec) for flyover conditions. The results of the investigation at a relative jet velocity of about 500 meters per second can be summarized as follows:

1. Comparison of the adjusted spectra at the acoustic angle that results in peak

flyover noise indicates that flight velocity had little effect on the suppression of the 48-tube primary. However, flight velocity adversely affects the noise suppression of the 48-tube primary with acoustically treated shroud and plug. Incorporating the scoops reduced the adverse effect a little.

2. The variation in perceived noise level with acoustic angle during a typical flyover of the 48-tube suppressor compared with that extrapolated from static data indicates that the static results correctly predicted both the peak noise level and the angle at which it occurred. This was not the case when the acoustic shroud and plug were installed. Then the static results predicted a higher peak value occurring farther away from the jet axis.

3. Peak noise level of the 48-tube suppressor in flyover was about the same as that of the baseline nozzle but occurred about 20° farther from the jet axis than for the baseline nozzle. (Peak noise level of the baseline nozzle was 115 PNdB occurring at an angle of 40°.) Incorporating the acoustic shroud and plug resulted in a substantial reduction of 9 PNdB and shifted the peak 40° closer to the jet axis when compared with the 48-tube primary. Scoops had a large effect on noise directivity but little effect on noise reduction.

4. The frequency spectrum for the 48-tube suppressor in flyover contains only a small amount of low-frequency noise but as much high-frequency noise as the baseline nozzle. The high-frequency noise peaks at a frequency of 4000 hertz. Incorporating the acoustic shroud reduced the noise level by as much as 14 decibels at a frequency of 4000 hertz.

5. When the acoustic data from the flyover were scaled from J85 engine size (0.23 scale) to full scale and extrapolated to a sideline distance of 648 meters (2128 ft) from an altitude of 305 meters (1000 ft), the 48-tube suppressor reduced the noise level by 5 EPNdB (relative to the baseline nozzle). This reduction was achieved with a thrust penalty of about 10.5 percent. The greatest amount of noise reduction, 15 EPNdB, was achieved by incorporating the scoops along with the acoustic shroud and plug. However, it was achieved with a thrust loss of 34 percent.

Lewis Research Center,
National Aeronautics and Space Administration,
Cleveland, Ohio, September 26, 1973,
501-24.

APPENDIX - SYMBOLS

A_8	primary nozzle exit effective flow area (hot), cm^2 ($in.^2$)
D	nozzle drag, kN (lbf)
D_b	base pressure drag, kN (lbf)
d_n	nacelle diameter, 63.5 cm (25 in.)
dB	decibel (re $2x10^{-5}$ N/m^2)
EPNL	effective perceived noise level, EPNdB
F	thrust, kN (lbf)
F_{ip}	ideal thrust of primary jet, kN (lbf)
M_0	flight Mach number
OASPL	overall sound pressure level, dB (re $2x10^{-5}$ N/m^2)
PNL	perceived noise level, PNdB
p_o	ambient static pressure, kN/m^2 (psia)
P_8	total pressure at primary nozzle exit, kN/m^2 (psia)
P_8/p_o	nozzle pressure ratio
R_p	direct ray distance between exhaust nozzle and microphone, m (ft)
r_β	boattail junction radius, cm (in.)
T_S	total temperature
T_8	total temperature at primary nozzle exit, K (^oR)
V_a	aircraft velocity, m/sec (ft/sec)
V_J	ideal jet velocity, m/sec (ft/sec)
V_r	relative jet velocity, $V_J - V_a$, m/sec (ft/sec)
W_S	secondary weight flow, kg/sec (lbm/sec)
W_8	weight flow at primary nozzle exit, kg/sec (lbm/sec)
θ	angle between direct ray and jet centerline, deg
$\omega\sqrt{\tau}$	corrected secondary weight flow ratio, $W_S/W_8 \sqrt{T_S/T_8}$

REFERENCES

1. Darchuk, George V.; and Balombin, Joseph R.: Noise Evaluation of Four Exhaust Nozzles for Afterburning Turbojet Engines. NASA TM X-2014, 1970.

2. Huff, Ronald G.; and Groesbeck, Donald E.: Splitting Supersonic Nozzle Flow into Separate Jets by Overexpansion into a Multilobed Divergent Nozzle. NASA TN D-6667, 1972.

3. Ciepluch, Carl C.; North, Warren J.; Coles, Willard D.; and Antl, Robert J.: Acoustic, Thrust, and Drag Characteristics of Several Full-Scale Noise Suppressors for Turbojet Engines. NACA TN 4261, 1958.

4. Brausch, J. F.: Flight Velocity Influence on Jet Noise of Conical Ejector, Annular Plug, and Segmented Suppressor Nozzles. General Electric Co. (NASA CR-120961), Aug. 1972.

5. Burley, Richard R.; and Karabinus, Raymond J.: Flyover and Static Tests to Investigate External Flow Effect on Jet Noise for Non-Suppressor and Suppressor Exhaust Nozzles. NASA TM X-68161, 1972.

6. Burley, Richard R.; Karabinus, Raymond J.; and Freedman, Robert J.: Flight Investigation of Acoustic and Thrust Characteristics of Several Exhaust Nozzles Installed on Underwing Nacelles on an F-106 Aircraft. NASA TM X-2854, 1973.

7. Chamberlin, Roger: Flyover and Static Tests to Study Flight Velocity Effects on Jet Noise of Suppressed and Unsuppressed Plug Nozzle Configurations. NASA TM X-2856, 1973.

8. Burley, Richard R.; and Johns, Albert L.: Flight Velocity Effects on Jet Noise of Several Variations of a Twelve-Chute Suppressor Installed on a Plug Nozzle. NASA TM X-2918, 1973.

9. Samanich, Nick E.; and Chamberlin, Roger: Flight Investigation of Installation Effects on a Plug Nozzle Installed on an Underwing Nacelle. NASA TM X-2295, 1971.

10. Mangiarotty, R. A.; Marsh, Alan H.; and Feder, Ernest: Duct-Lining Materials and Concepts. Progress of NASA Research Relating to Noise Alleviation of Large Subsonic Jet Aircraft. NASA SP-189, 1968, pp. 29-52.

11. Groth, Harold W.; Samanich, Nick E.; and Blumenthal, Philip Z.: Inflight Thrust Measuring System for Underwing Nacelles Installed on a Modified F-106 Aircraft. NASA TM X-2356, 1971.

12. Antl, Robert J.; and Burley, Richard R.: Steady-State Airflow and Afterburning Performance Characteristics of Four J85-GE-13 Turbojet Engines. NASA TM X-1742, 1969.

13. Little, John W.; Miller, Robert L.; Oncley, Paul B.; and Panko, Raymond E.: Studies of Atmospheric Attenuation of Noise. NASA Acoustically Treated Nacelle Program. NASA SP-220, 1969, pp. 125-135.

14. Grande, E.: Exhaust Noise Field Generated in the JT8D Core Engine - Noise Floor Presented by the Internal Noise Source. Presented at the Acoustical Society of America 82nd Fall Meeting, Denver, Colo., Oct. 19-22, 1971.

15. Anon.: Jet Noise Prediction. Aerospace Information Rep. 876, SAE, July 10, 1965.

16. Anon.: Federal Aviation Regulations, Vol. III, Part 3b, Noise Standards: Aircraft Type Certification. Dept. of Transportation, Federal Aviation Administration.

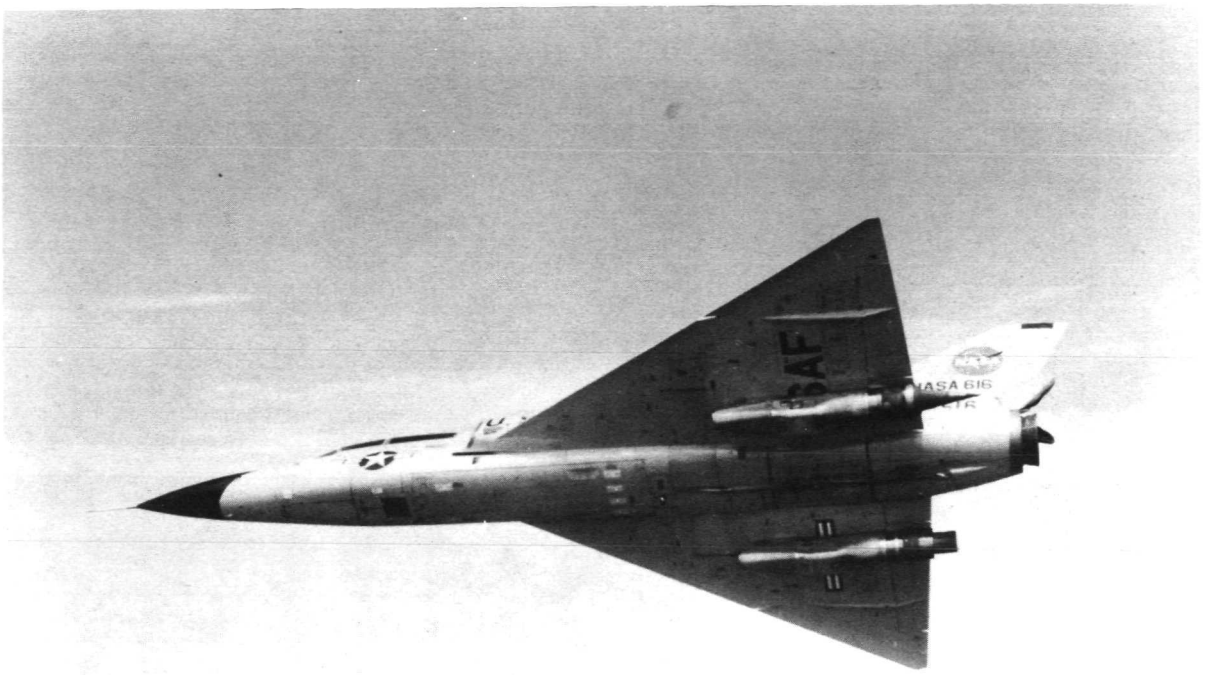

C-69-2871

Figure 1. - Modified F-106B aircraft in flight.

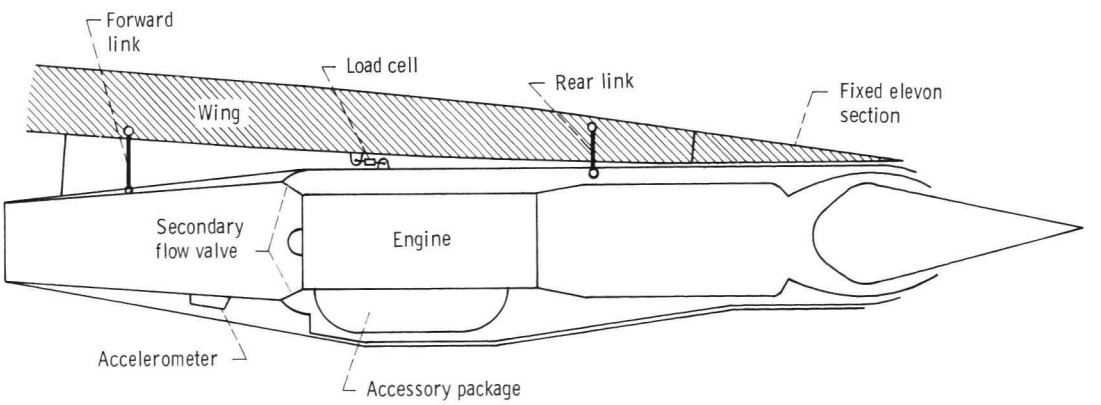

Figure 2. - Nacelle-engine installation.

Figure 3. - Nacelle modification for static tests.

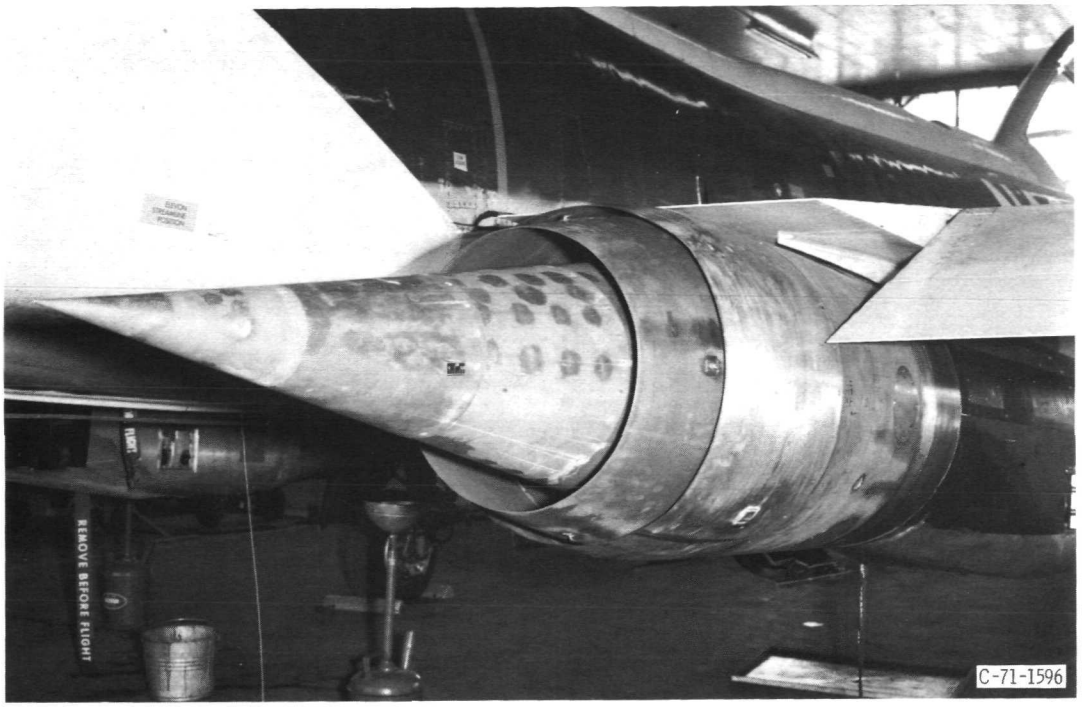

(a) Installed.

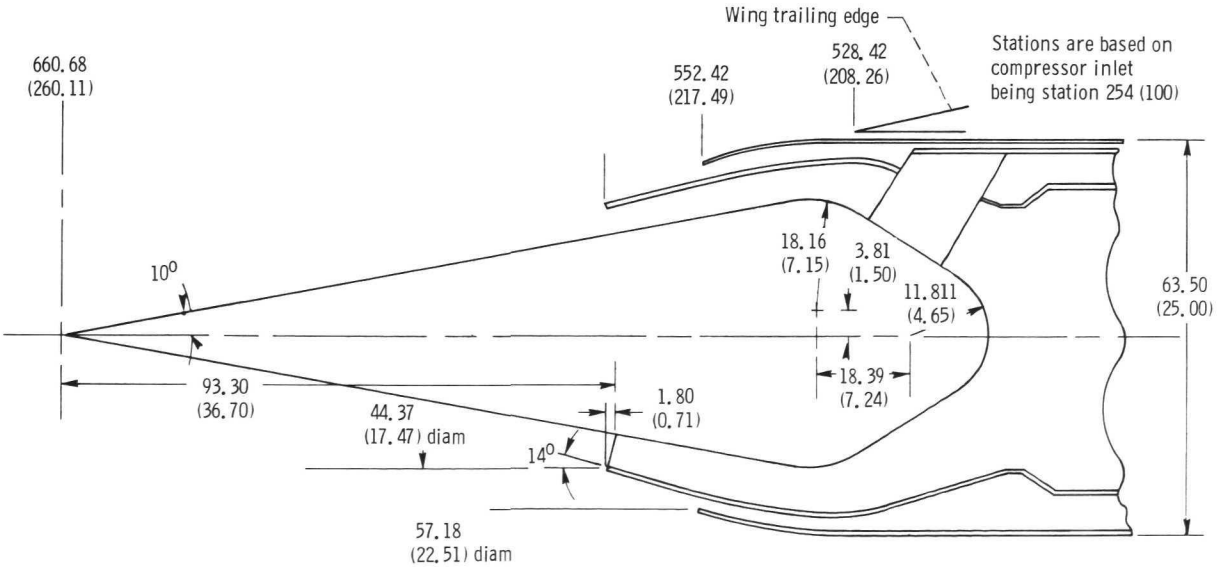

(b) Dimensional characteristics. (Dimensions are in cm (in.).)

Figure 4. - Baseline nozzle.

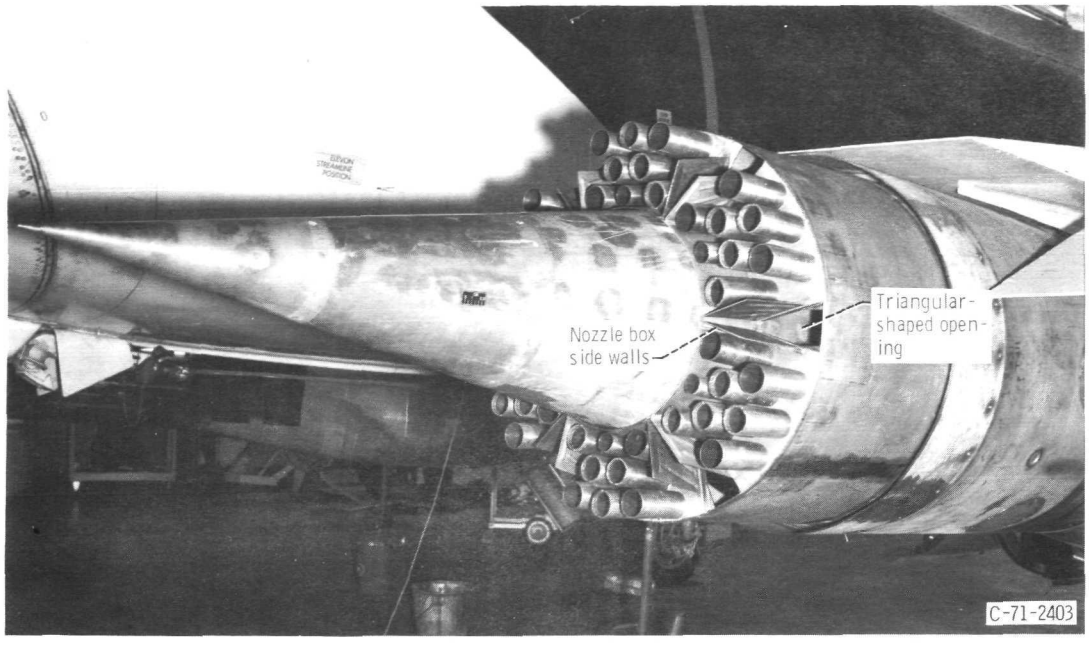

(a-1) Installed.

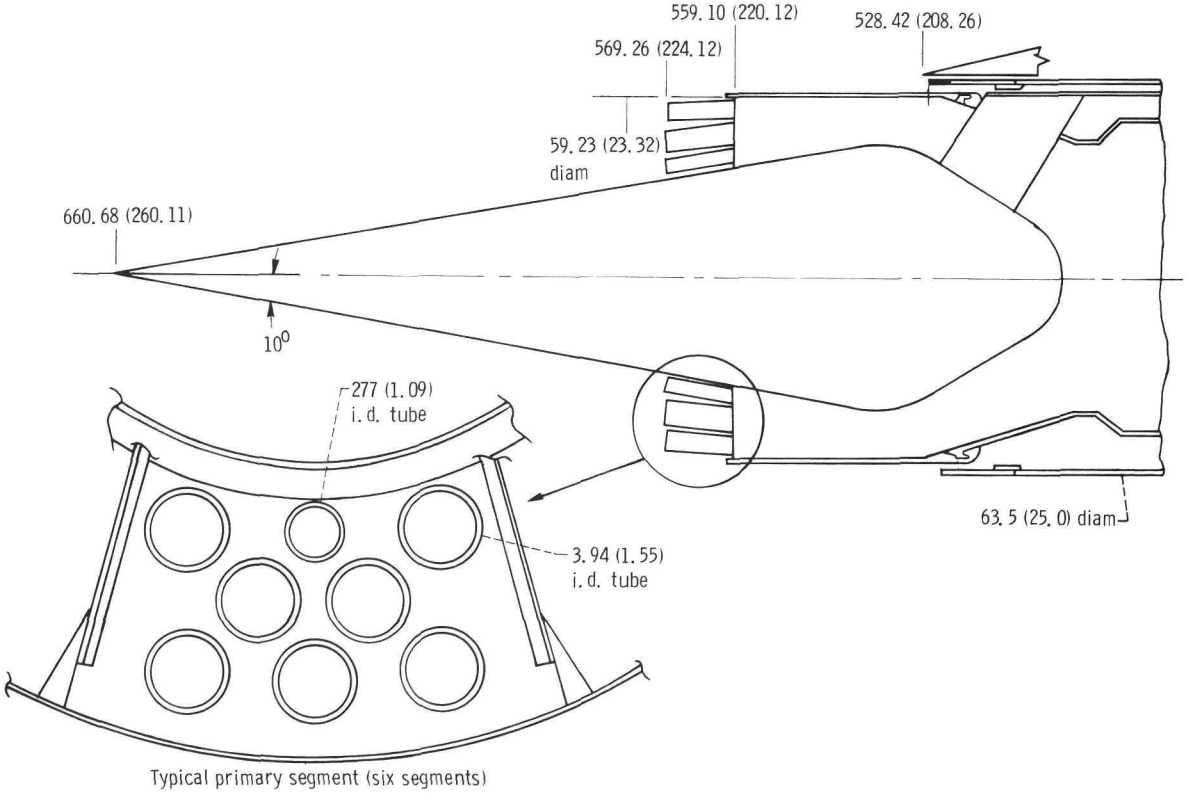

(a-2) Dimensional characteristics. Dimensions are in centimeters (in.).

(a) 48-Tube primary.

Figure 5. - Forty-eight-tube suppressor configurations.

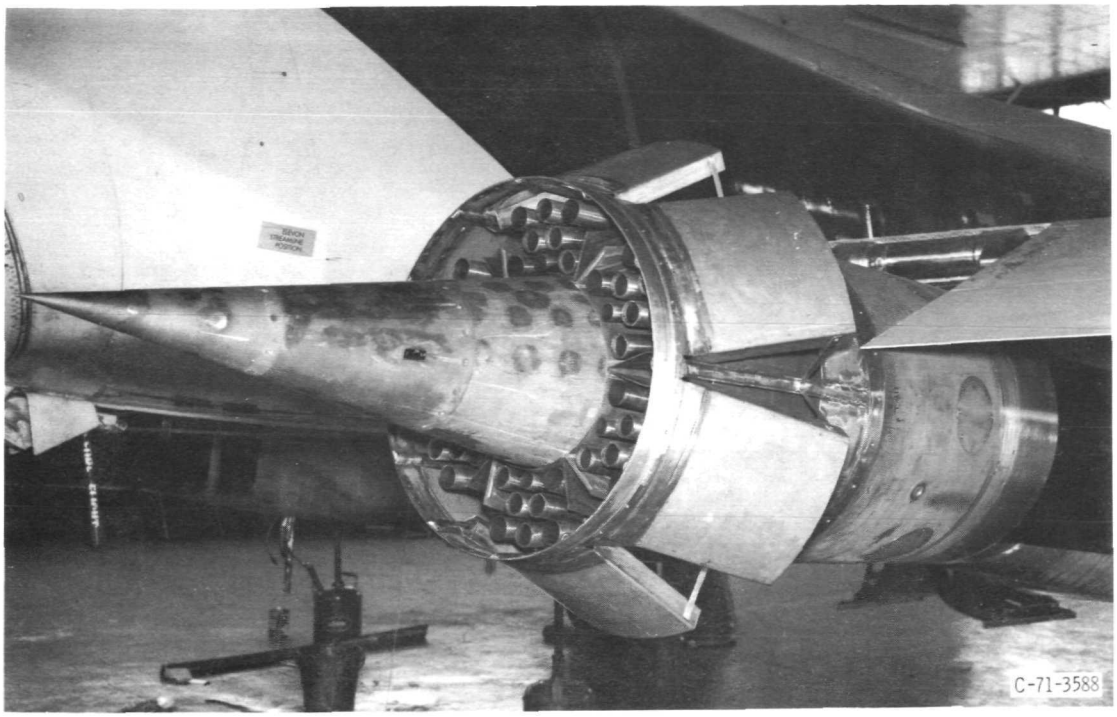

(b-1) Installed.

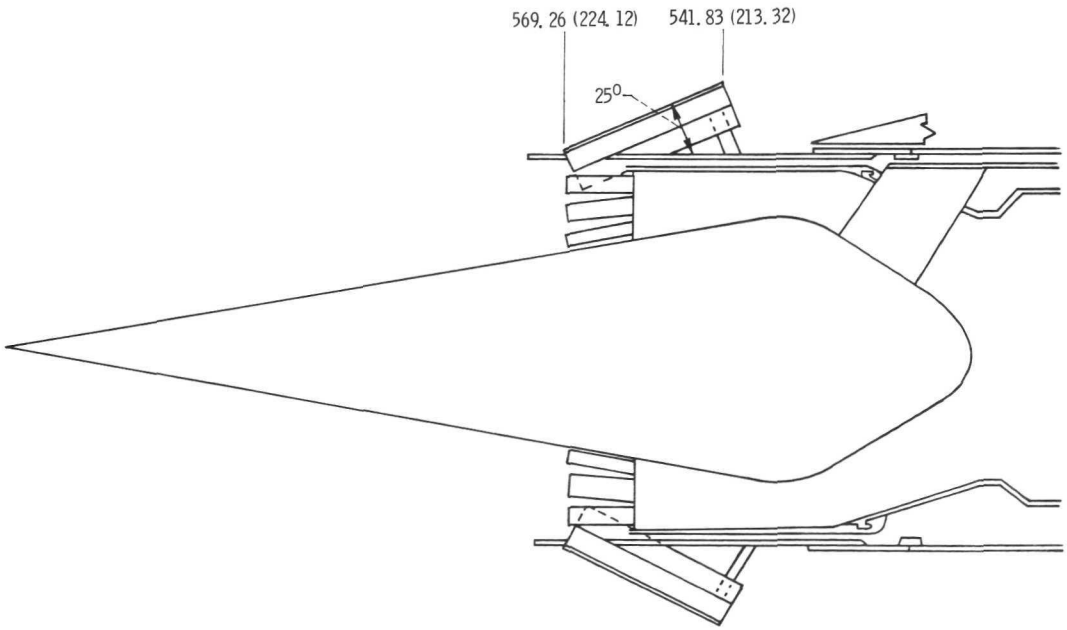

(b-2) Dimensional characteristics. (Dimensions are in cm (in.).)

(b) 48-Tube primary with scoops.

Figure 5. - Continued.

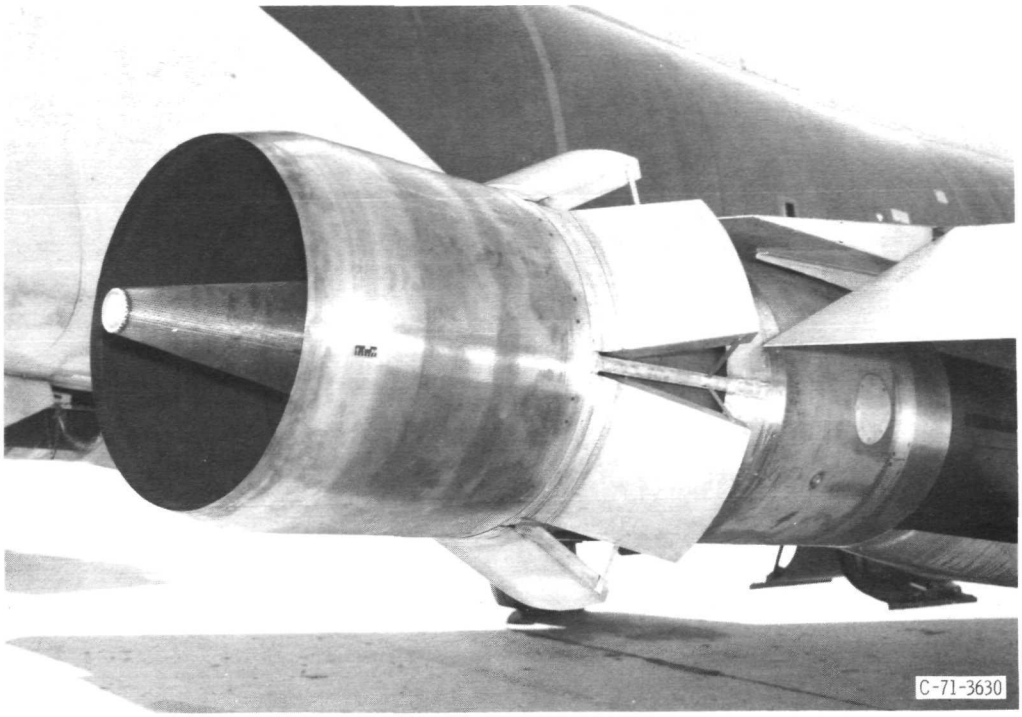

(c-1) Installed.

Perforated plate				
Open area ratio	Hole diameter		Thickness	
	cm	in.	cm	in.
0.23	0.198	0.078	0.079	0.0312

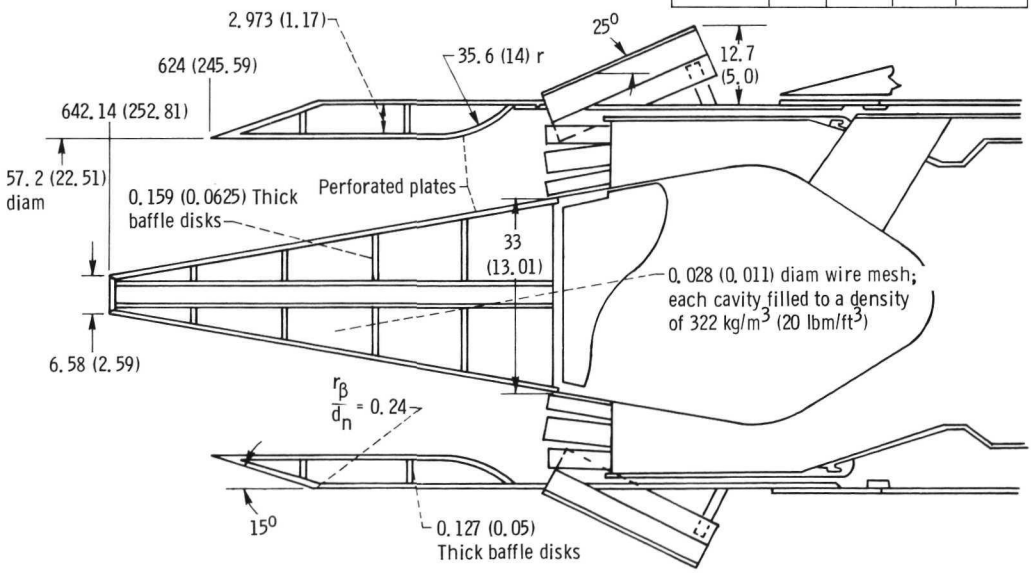

(c-2) Dimensional characteristics. Dimensions are in centimeters (in.). (These components comprise three configurations: as shown, without scoops, with plain plug instead of acoustic plug.)

(c) 48-Tube primary with tubes plus acoustic shroud and acoustic plug.

Figure 5. - Concluded.

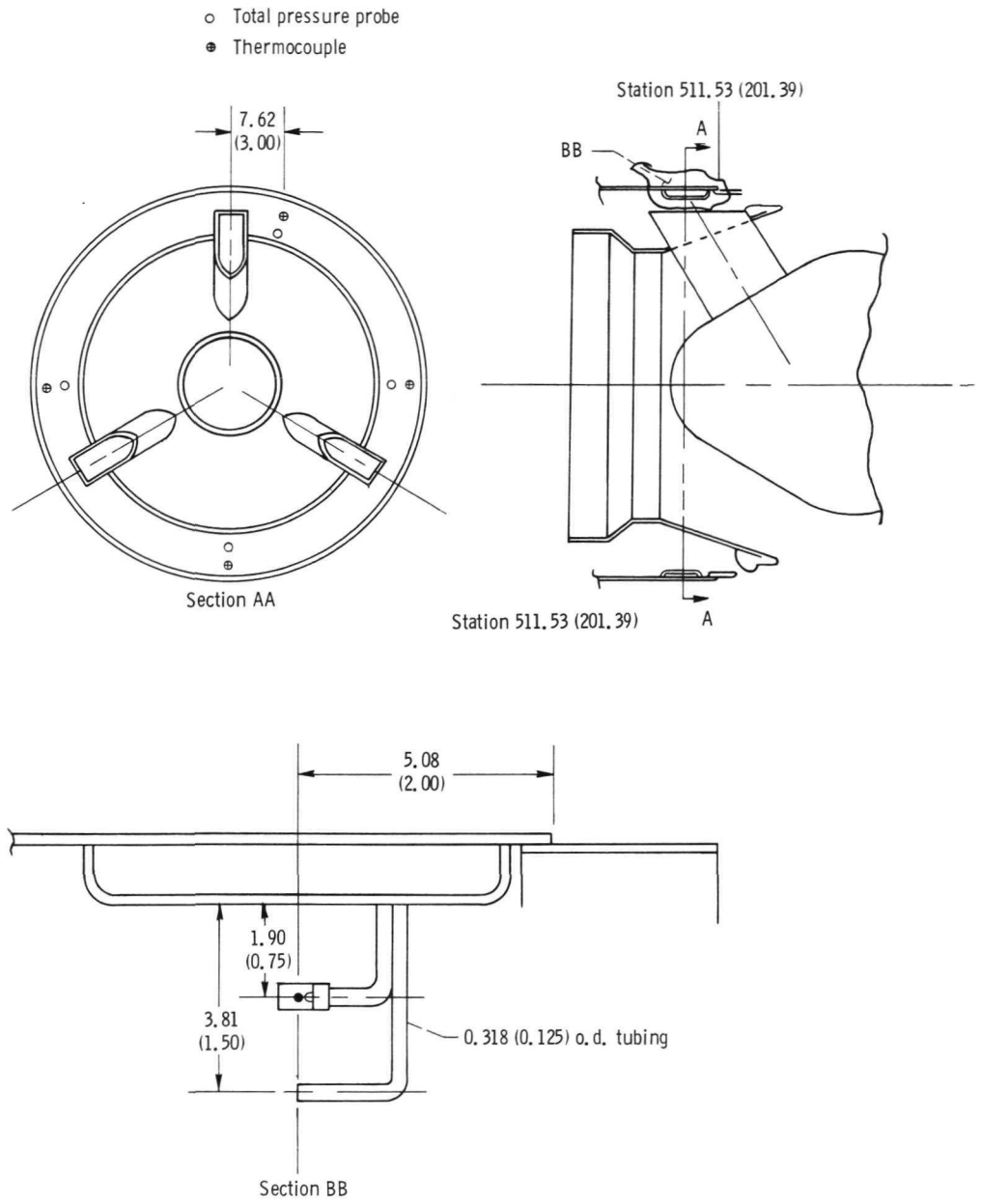

Figure 6. - Secondary passage instrumentation. (Dimensions are in cm (in.).)

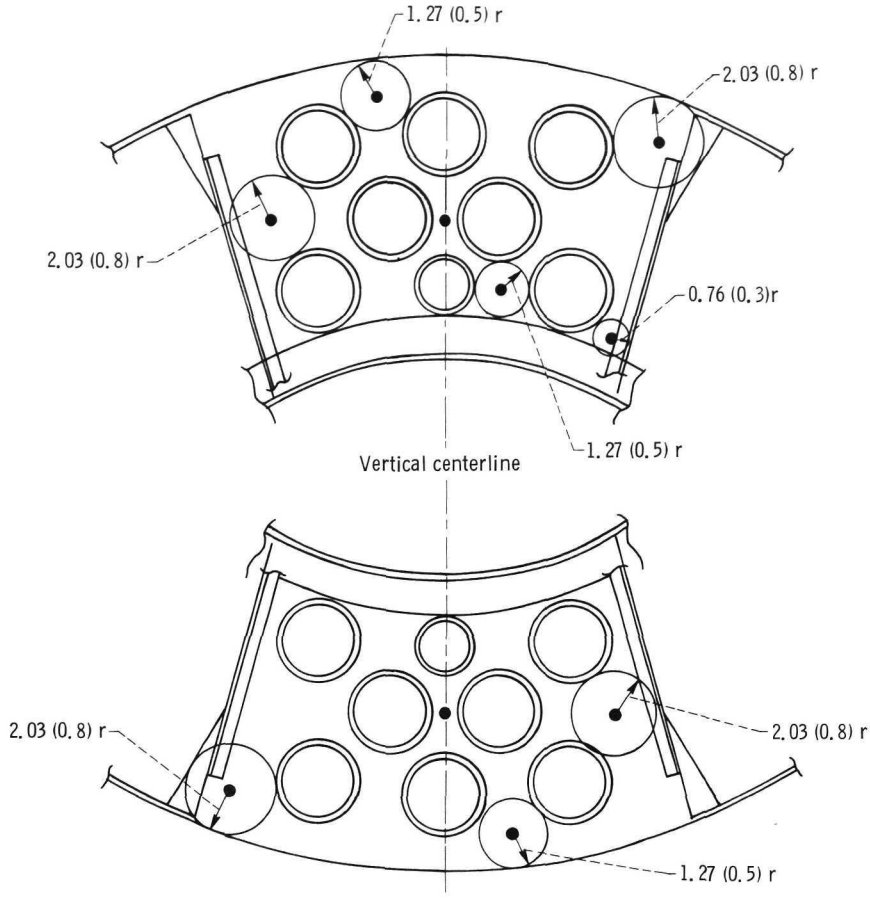

Multitube primary (looking upstream); station 559.1 (220.12)

Figure 7. - Primary base static pressure instrumentation. Dimensions are in centimeters (in.).

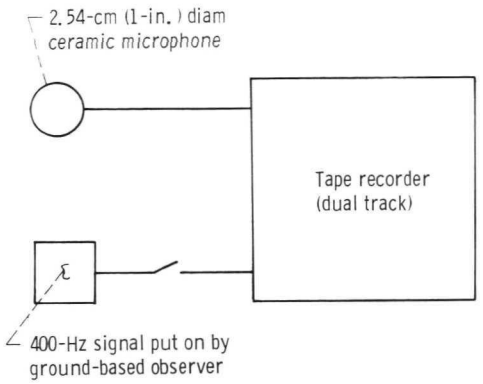

(a) Recording system for both static and flyover tests.

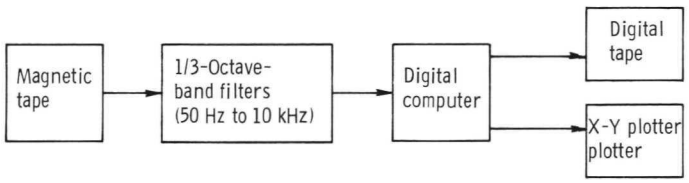

(b) Playback system for flyover tests.

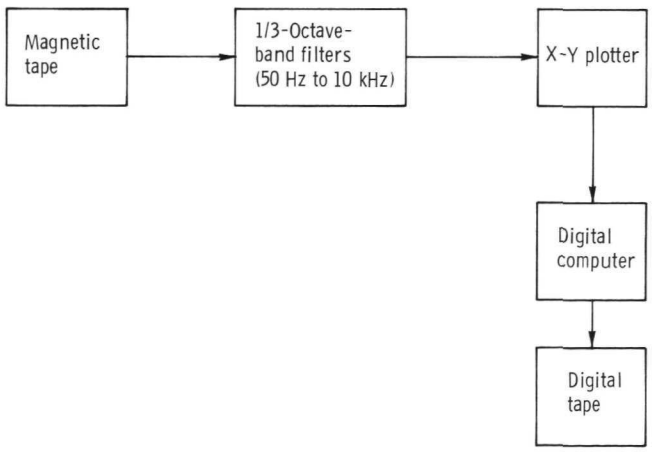

(c) Playback system for static tests.

Figure 8. - Schematic flow diagrams for noise recording system and data reduction for both static and flyover.

(a) Microphone orientation.

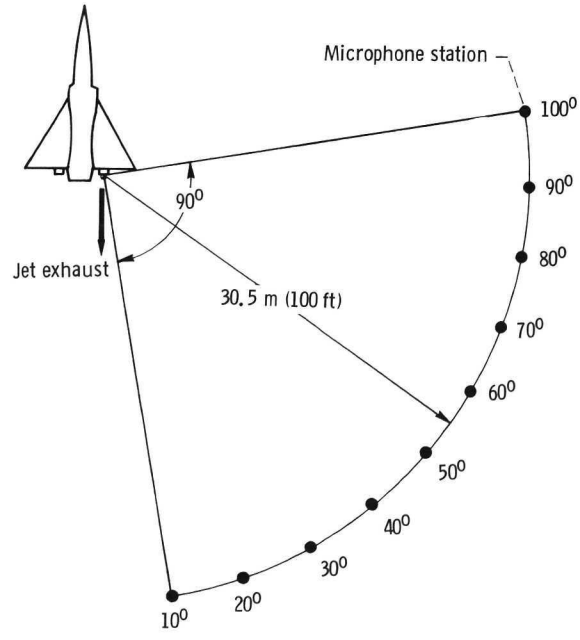

(b) Microphone location.

Figure 9. - Microphone orientation and location for static tests.

Figure 10. - Location of external source of cooling air for static tests.

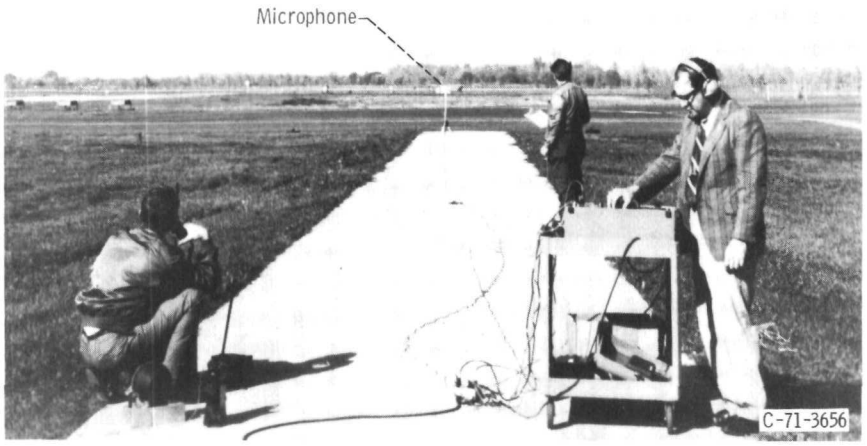

(a) Microphone orientation.

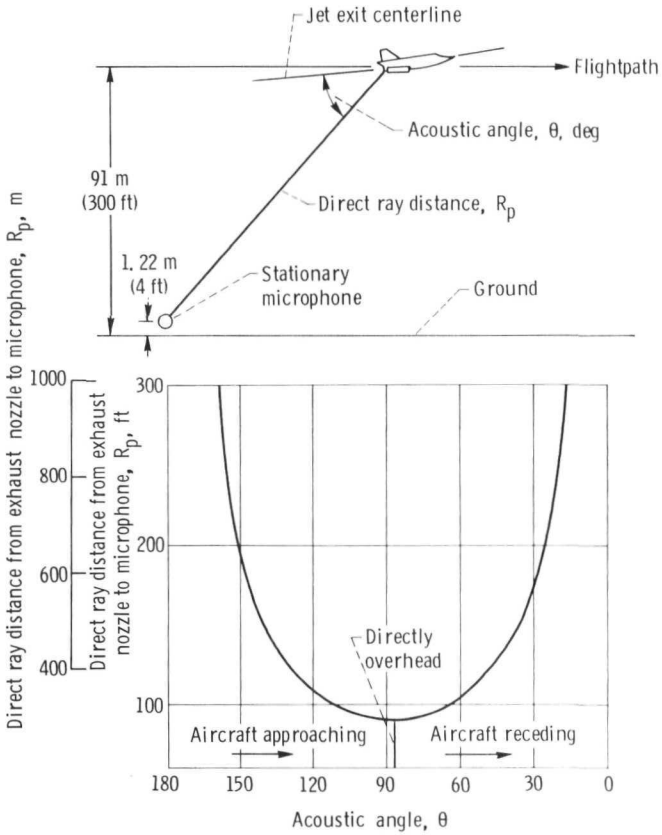

(b) Geometry.

Figure 11. - Microphone orientation and geometry for flyover tests.

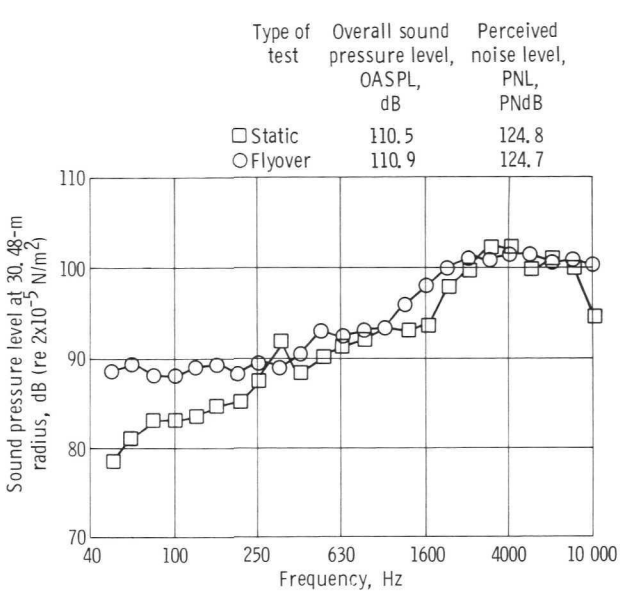

Figure 12. - Comparison of flyover and static spectra for 48-tube suppressor nozzle. Relative jet velocity, V_r, 504 m/sec (1654 ft/sec); angle of peak noise flyover (acoustic angle), θ, 70^0; 1/3-octave bands.

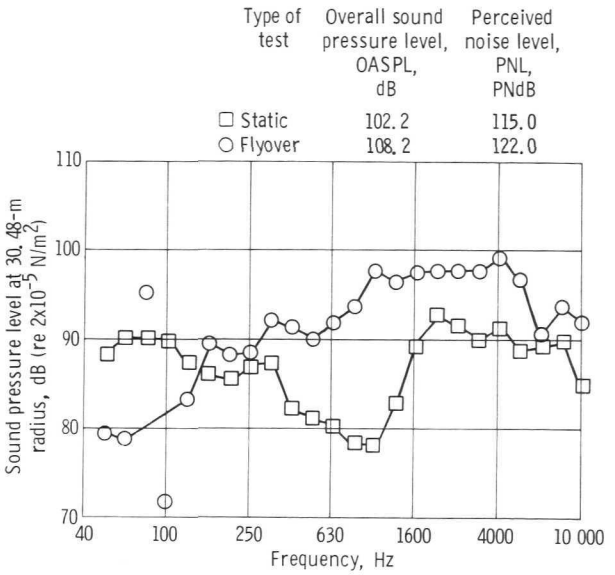

Figure 13. - Comparison of flyover and static spectra for 48-tube suppressor nozzle with acoustic shroud and acoustic plug. Relative jet velocity, V_r, 501 m/sec (1644 m/sec); angle of peak noise for flyover (acoustic angle), θ, 30^0; 1/3-octave bands.

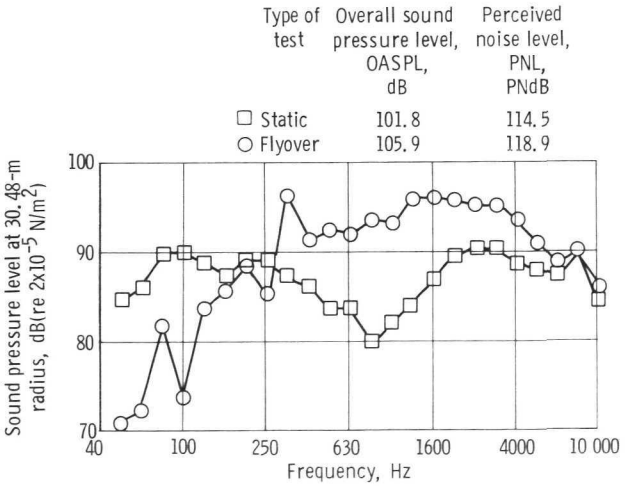

Figure 14. - Comparison of flyover and static spectra for 48-tube suppressor nozzle with scoops plus acoustic shroud and plug. Relative jet velocity, V_r, 501 m/sec (1642 ft/sec); angle of peak noise for flyover (acoustic angle), θ, 30^0; 1/3-octave bands.

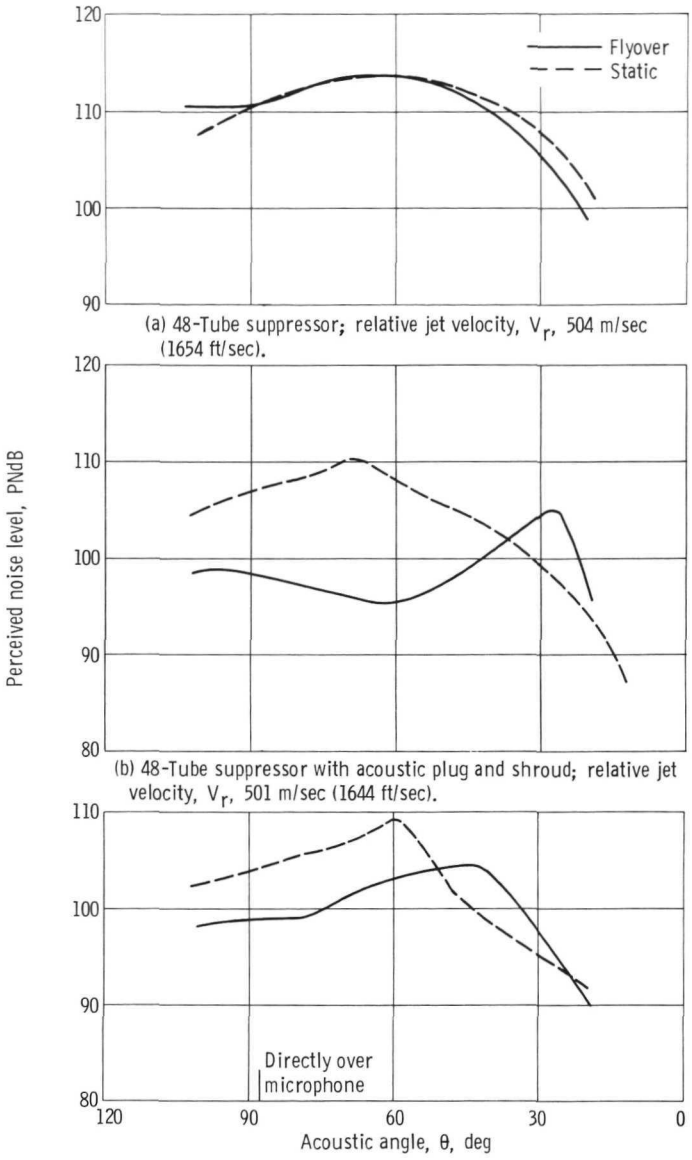

(a) 48-Tube suppressor; relative jet velocity, V_r, 504 m/sec (1654 ft/sec).

(b) 48-Tube suppressor with acoustic plug and shroud; relative jet velocity, V_r, 501 m/sec (1644 ft/sec).

(c) 48-Tube suppressor with scoops plus acoustic plug and acoustic shroud; relative jet velocity, V_r, 501 m/sec (1642 ft/sec).

Figure 15. - Flyover and static noise directivity. Comparison of flyover data at 91-meter altitude with static data extrapolated to a 91-meter sideline. Data adjusted to free-field and standard-day conditions.

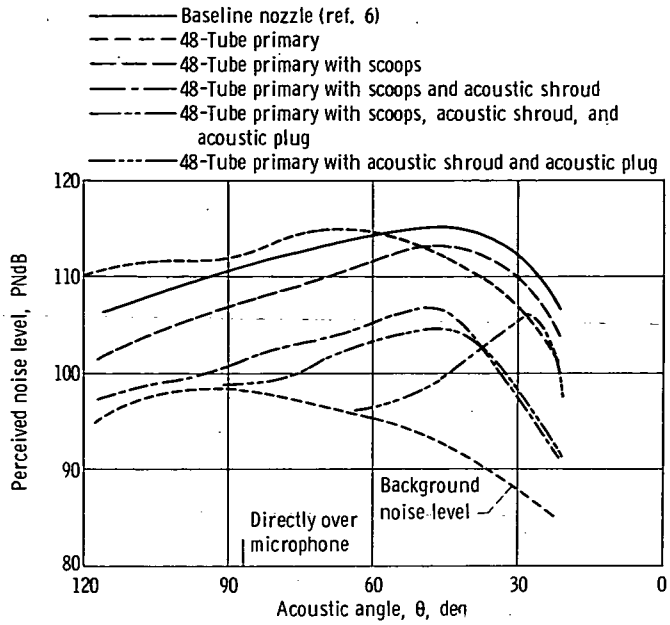

Figure 16. - Flyover noise levels directly beneath flightpath. Data adjusted to free-field, standard-day conditions. Altitude, 91 m; relative jet velocity, V_r, 502 m/sec (1646 ft/sec).

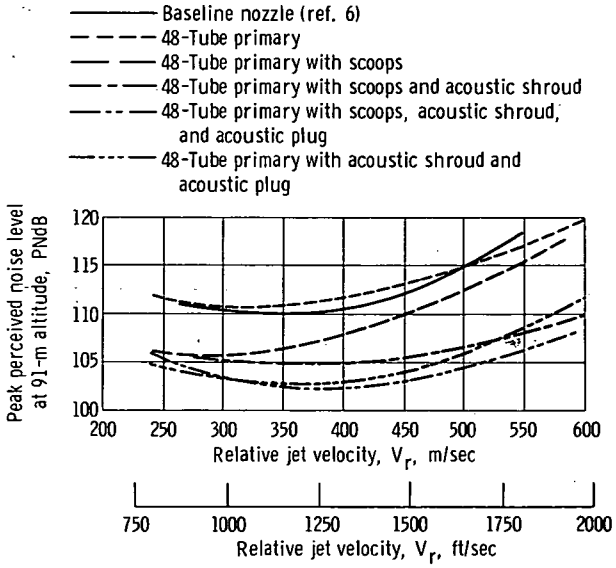

Figure 17. - Effect of relative jet velocity on peak flyover noise levels.

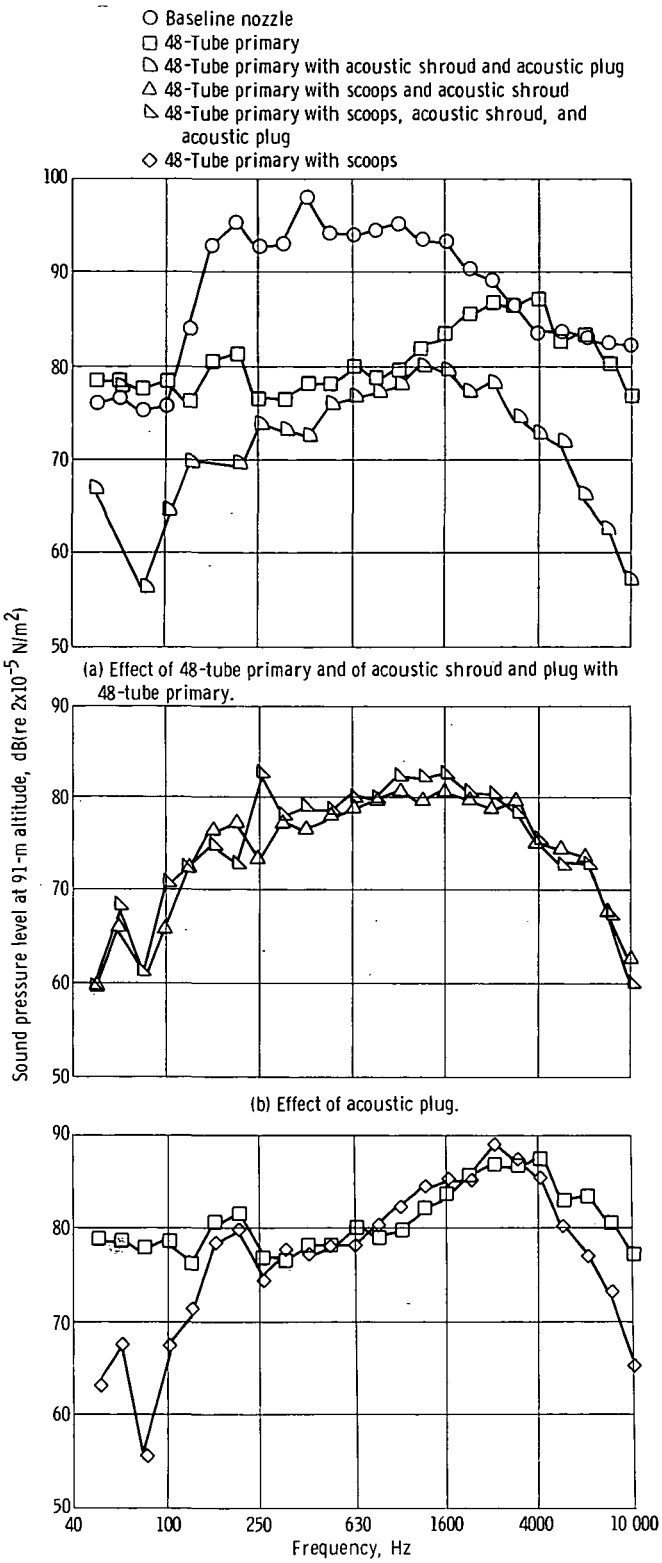

(a) Effect of 48-tube primary and of acoustic shroud and plug with 48-tube primary.

(b) Effect of acoustic plug.

(c) Effect of scoops on 48-tube primary.

Figure 18. - Comparison of flyover spectra. Relative jet velocity, V_r, 502 m/sec (1646 ft/sec); acoustic angle (angle of peak noise for plug at flyover), θ, 40^0; 1/3-octave bands.

Configuration	Ratio of base pressure drag to ideal thrust of primary jet,[a] D_b/F_{ip}
48-Tube primary	0.022
48-Tube primary with acoustic shroud and acoustic plug	.078

[a]At $P_8/p_0 = 2.1$

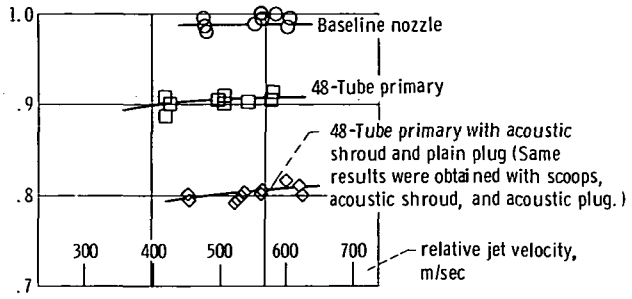

(a) Static tests.

Configuration	Ratio of base pressure drag to ideal thrust of primary jet,[a] D_b/F_{ip}
48-Tube primary	0.06
48-Tube primary with scoops	.078
48-Tube primary with scoops and acoustic shroud	.142

[a]At $P_8/p_0 = 2.4$

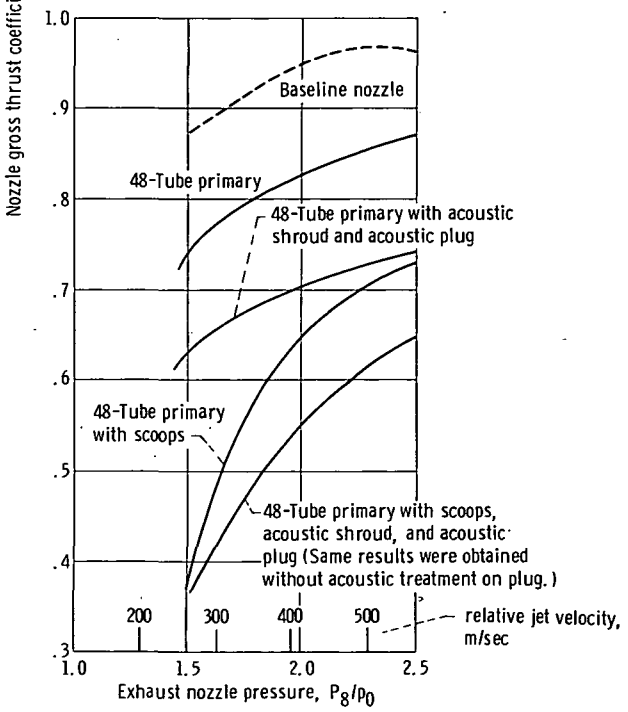

(b) Flyover tests. Flight Mach number, M_0, 0.4; corrected secondary weight flow ratio, $\omega\sqrt{\tau}$, 0.06.

Figure 19. - Thrust performance of suppressor configurations relative to baseline nozzle.

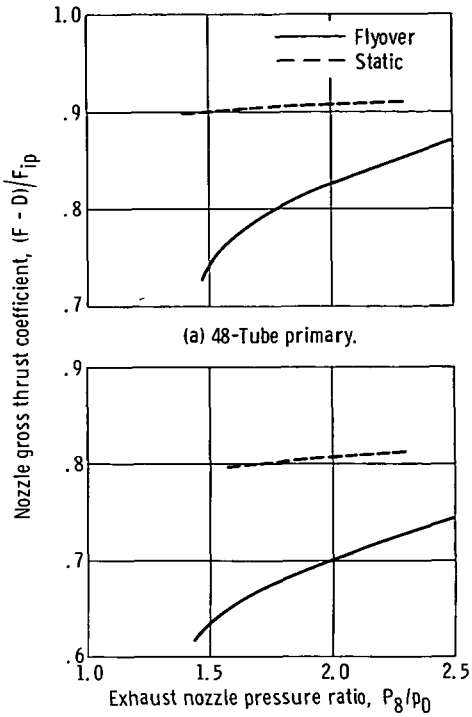

(b) 48-Tube primary with acoustic shroud and acoustic plug.

Figure 20. - Effect of flight velocity on thrust of suppressor configurations.

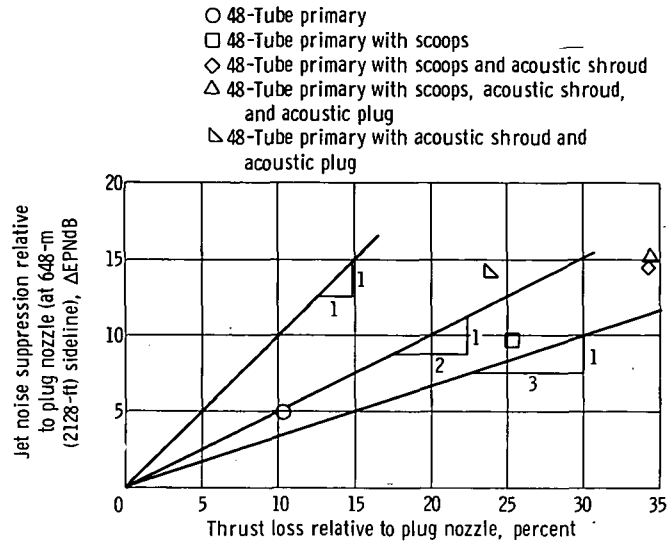

Figure 21. - Suppressor effectiveness. Flyover results scaled to four 267-kN-thrust engines; exhaust nozzle pressure ratio, P_8/p_0, 2.4; relative jet velocity, V_r, 533 m/sec (1750 ft/sec); corrected secondary rate flow ratio $\omega\sqrt{\tau}$, 0.06, Flight Mach number, M_0, 0.4.

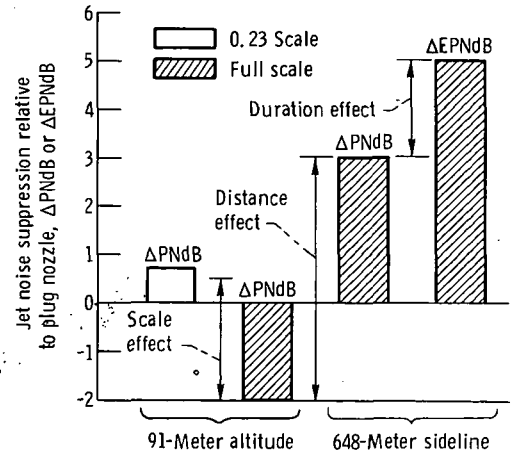

Figure 22. - Effect of scale, distance, and duration on suppression of 48-tube primary.

Page Intentionally Left Blank

NATIONAL AERONAUTICS AND SPACE ADMINISTRATION
WASHINGTON, D.C. 20546

OFFICIAL BUSINESS
PENALTY FOR PRIVATE USE $300

SPECIAL FOURTH-CLASS RATE
BOOK

POSTAGE AND FEES PAID
NATIONAL AERONAUTICS AND
SPACE ADMINISTRATION
451

U.S.MAIL

POSTMASTER : If Undeliverable (Section 158 Postal Manual) Do Not Return

"The aeronautical and space activities of the United States shall be conducted so as to contribute . . . to the expansion of human knowledge of phenomena in the atmosphere and space. The Administration shall provide for the widest practicable and appropriate dissemination of information concerning its activities and the results thereof."

—NATIONAL AERONAUTICS AND SPACE ACT OF 1958

NASA SCIENTIFIC AND TECHNICAL PUBLICATIONS

TECHNICAL REPORTS: Scientific and technical information considered important, complete, and a lasting contribution to existing knowledge.

TECHNICAL NOTES: Information less broad in scope but nevertheless of importance as a contribution to existing knowledge.

TECHNICAL MEMORANDUMS: Information receiving limited distribution because of preliminary data, security classification, or other reasons. Also includes conference proceedings with either limited or unlimited distribution.

CONTRACTOR REPORTS: Scientific and technical information generated under a NASA contract or grant and considered an important contribution to existing knowledge.

TECHNICAL TRANSLATIONS: Information published in a foreign language considered to merit NASA distribution in English.

SPECIAL PUBLICATIONS: Information derived from or of value to NASA activities. Publications include final reports of major projects, monographs, data compilations, handbooks, sourcebooks, and special bibliographies.

TECHNOLOGY UTILIZATION PUBLICATIONS: Information on technology used by NASA that may be of particular interest in commercial and other non-aerospace applications. Publications include Tech Briefs, Technology Utilization Reports and Technology Surveys.

Details on the availability of these publications may be obtained from:

SCIENTIFIC AND TECHNICAL INFORMATION OFFICE

NATIONAL AERONAUTICS AND SPACE ADMINISTRATION

Washington, D.C. 20546